19th International Symposium of Ballistics, 7–11 May 2001, Interlaken, Switzerland

BREAKUP OF SHAPED-CHARGE JETS: COMPARISON BETWEEN EXPERIMENTAL AND NUMERICAL DATA

M.D. Rodriguez[1], V. Jeanclaude[2], J. Petit[3] and C. Fressengeas[2]

[1] *Universidad de Valladolid, Valladolid 47011, Spain*
[2] *L.P.M.M., Université de Metz / C.N.R.S., Ile du Saulcy, 57045 Metz, France*
[3] *Centre d'Etudes de Gramat, 46500 Gramat, France*

The particulation of a shaped-charge jet is modeled as the axisymmetric dynamic necking instability of a viscoplastic metallic material. Analytical / numerical predictions are obtained from a linear perturbation analysis for the jet break-up time, the fragments velocity and aspect ratio. Comparisons are attempted with experimental data obtained from flash radiographs of copper jets. Rugosity measurements carried out on intact recovered fragments provide realistic estimates for the geometrical imperfections of the jets. Despite the simplicity of the model, a good agreement between theoretical and experimental data is obtained when using typical values of the strength and strain rate sensitivity of copper at high strain rates.

INTRODUCTION

High speed metallic jets produced by shaped-charge devices experience very large amounts of stretching during their flight. However their length is limited by particulation, a process detrimental to their perforating capabilities. The physical origin of this phenomenon has been investigated for more than 50 years [1–7]. It is now generally agreed that particulation pertains to necking instabilities. Hydrocode simulations of this necking process are commonly used to provide predictions that could be compared to experimental observations. In particular, such calculations have lead to estimates of the yield strength of the material in jet conditions [8]. Simpler analytical models are still needed. By selecting the essential features, they provide a basic understanding of the phenomenon. Trends and limits can be displayed when material and geometrical parameters are varied, and quantitative estimates may also be obtained, at negligible expense. In the present paper, a model accounting for the features of the dynamic necking process in a viscoplastic material is used to predict the influence of various material and experimental parameters, as well as to provide reasonably accurate quantitative results.

Home
Table of Contents

MODEL FORMULATION

This section provides a brief outline of the model used in the present work. For a more detailed account, the reader is referred to ref. [9]. Initial conditions to the model jet are such that the axial velocity distribution is linear along its extent L. Velocity boundary conditions are imposed at the ends of the jet: the velocity V of the jet tip relative to its rear end is supposed constant. In addition, stress-free lateral edges and axial symmetry are assumed. In the extreme jet strain rate conditions, the material behavior is taken to be visco-plastic. Strain hardening, anisotropy and thermal coupling are neglected. If $\boldsymbol{D}$ is the strain rate tensor, $\boldsymbol{s}$ the Cauchy stress tensor deviator, σ_e the equivalent von Mises stress and D_e the equivalent strain rate, the constitutive relations are

$$\boldsymbol{s} = \Lambda \boldsymbol{D}, \quad \Lambda = \frac{2}{3}\frac{\sigma_e}{D_e}, \quad \sigma_e = \eta D_e^m \tag{1}$$

m denotes the material strain rate sensitivity. At the large strain rates encountered in the jets, m ranges from 0.01 below 10^3 s^{-1} to 0.2 at 2.10^4 s^{-1}. From the experimental data reported in [10], a reasonable value amounts to 0.05 at 10^4 s^{-1}. Taken as a constant, this value is used in the rest of the paper. The Lagrangian momentum equations are

$$\rho \frac{\partial \boldsymbol{v}}{\partial t} = div\, \boldsymbol{n} \tag{2}$$

where $\boldsymbol{n}$ is the Boussinesq (non symmetric) stress tensor. $\boldsymbol{F}$ being the deformation gradient, the Boussinesq and Cauchy stress tensors ($\boldsymbol{n}$, σ) are related through

$$\boldsymbol{n} = J\sigma \boldsymbol{F}^{-t}, \quad J = \det \boldsymbol{F} = 1 \tag{3}$$

Incompressibility being assumed, J is equal to unity.

A uniform stretching of the jet is solution to eqs. (1–3) under the prescribed initial and boundary conditions. One prominent feature of that solution is radial unsteadiness: the radial velocity of particles decreases as they approach the jet centerline. As a result the material is subjected to an inertial radial pressure. Under the high strain rate conditions pertaining to shaped-charge jets, this pressure can be larger than the reference (flow) stress of the material σ^* (i.e. is the initial uniform tension stress). Such conditions are characterized by a Reynolds number $R_0 = \rho V^2 / \sigma^*$ larger than 1. Following [8], the estimate $\sigma^* = 0.1\ GPa$ will be used hereafter.

To investigate the instability of that uniform stretching solution, linear non uniform perturbations are superimposed. First order perturbation terms are retained in eqs. (1, 2, 3) and in boundary conditions. The perturbations are given in Fourier modes in the Lagrangian initial configuration. Further on they stretch with the material. The attention is focused on the Eulerian radius r of the jet cross-sections. If r_0 denotes its uniform value (as given by the uniform stretching solution), the amplification $a = (r_0 - r) / r_0$ is a measure of the jet non-uniformity. Since it is relative to r_0, this measure is more significant of non-

Home
Table of Contents

uniformity than the absolute measure $(r_0 - r)$ when deformations become large. Consider in addition the relative rate of growth G of a cross-section

$$G = m\dot{a} / a \tag{3}$$

G is normalized in the sense that its value is $G=1$ in a 1D quasi-static long wavelength reduction of the model. Clearly, non uniformity increases when $G>0$. In our model, G is obtained in closed form as a function of time and experimental parameters, provided that the rate of growth of the disturbances is much larger than the characteristic strain rate V/L of the uniform stretching. In quasi-static conditions, this result reduces to those of refs. [12, 13] and in dynamic long wave length conditions to the results of [11]. Clearly, the amplification a follows from the integration of relation (3) in time

$$a(t) = a(0)\exp\left(\frac{1}{m}\int_{\tau=0}^{\tau=t} G(\tau)d\tau\right) \tag{4}$$

$a(0)$ is a measure of the initial imperfections in the jet uniformity. In this work, $a(0)$ is estimated from measurements carried out on intact recovered fragments. The breakup time can be defined as the time t_b when at least one cross-section satisfies $a(t_b) = 1$. It should be clear that this breakup criterion is merely a linear extrapolation. Non linear failure mechanisms such as shear banding, which may occur at jet breakup [4], are not accounted for. Therefore the result obtained from this criterion is an overestimate of the actual breakup time. Nevertheless, since linear and nonlinear mechanisms are both destabilizing, it is likely to be reasonably close to the latter, particularly so when the perturbation growth rate is large.

MODEL RESULTS

The rate of growth G of the non uniformity, as given by eq. (3), is plotted at the initial time in Fig. 1 versus the perturbation wave number for various Reynolds numbers. G is always positive, meaning that the uniform stretching of the jet is unstable at all perturbation wave numbers. G is also less than 1. Thus inertia delays the growth of the non uniform disturbances. At long wave lengths (short wave numbers) the rate of growth G merges with the 1D dynamic approximation [11], and at short wave lengths with the quasi-static approximation [13]. Therefore inertia stabilizes significantly the uniform stretching with respect to long wave length perturbations only. As a result a wave number k_c of maximum perturbation growth is selected. After integration in time, the associated amplification provides information on the characteristic fragment length.

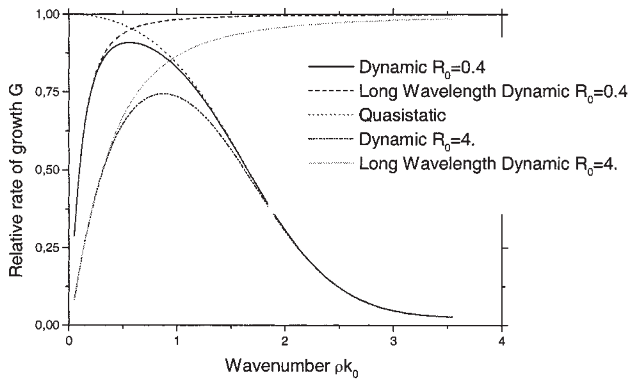

Figure 1: Dispersion curves at initial time; influence of inertia (m=0.05).

Fig. 1 also shows that the larger the Reynolds number R_0, the shorter the wavelength of maximum growth. Consequently more inertia leads to shorter fragments at the outcome of the process. The influence of rate sensitivity on the rate of growth G is plotted in Fig. 2. It is seen that increasing the rate sensitivity leads to smaller critical wave numbers. As a consequence, fragments will be larger at the end of the process in more rate sensitive materials.

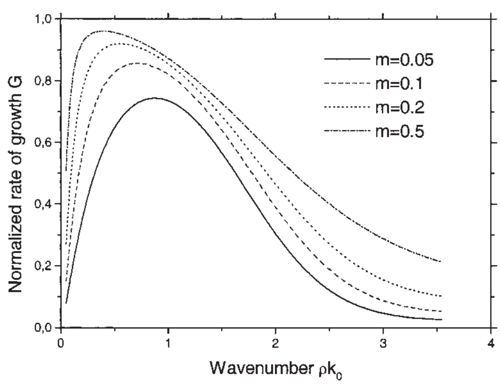

Figure 2: Influence of rate sensitivity on initial dispersion curve (Reynolds number R_0=4.).

The evolution in time of the dispersion curve shown in Fig. 1 for the Reynolds number R_0=4 is plotted in Fig. 3. It is seen that short wave length perturbations grow more rapidly than believed on the basis of the initial values, whereas the damping effects of radial inertia on long wave lengths are more and more effective. The figure also shows that the critical wave number k_c is shifted to larger values as time goes on, which reflects the sharpening of necking. The implication is that initially dominant modes may not be those who finally shape the jet non uniformity. As shown by performing the integration (4), the latter are actually those leading to the shortest breakup time.

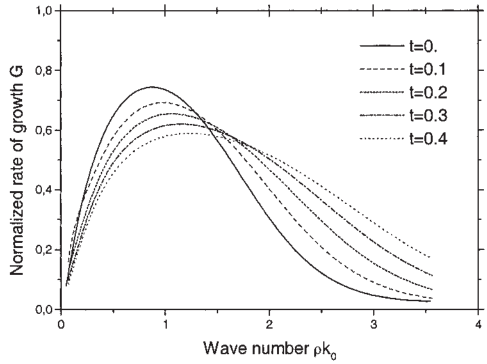

Figure 3: Time evolution of dynamic dispersion curve of Fig. 1 (Reynolds number R_0=4, m=0.05, non dimensional time).

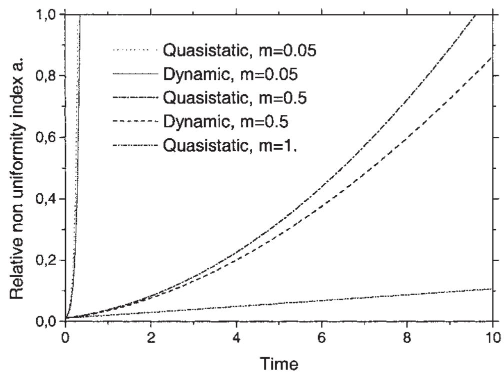

Figure 4: Amplification index a versus time, for a given wave number.

The amplification a is plotted in Fig. 4 in various conditions. A comparison of its growth in the quasi-static and dynamic cases (for the rate sensitivities $m=0.05$ and $m=0.5$) provides additional evidence that inertia delays the growth of non uniform disturbances. Comparing the amplification growth for identical Reynolds numbers but for different strain rate sensitivities ($m=0.05$, $m=0.5$, $m=1$ in quasi-static conditions) does show a dramatic increase in the rate of growth of the perturbations as rate sensitivity decreases, as well as much shorter breakup times. Thus, our assumption of rapid perturbation growth is all the more satisfied that rate sensitivity is smaller. We checked that the copper rate sensitivity $m=0.05$ is sufficiently small for the model to be unambiguously valid.

The model therefore implies the following trends. Jet materials with higher rate sensitivity yield larger breakup times and larger fragments. Jet materials with lower strength or higher density (i.e. higher inertia) yield larger breakup times but shorter fragments. These predictions are in agreement with common wisdom obtained from experimental data and nonlinear computations.

Home
Table of Contents

EXPERIMENTS AND DATA ANALYSIS

Comparisons between the model quantitative predictions and typical experimental data are now attempted on the basis of shaped-charge experiments first described in ref. [14]. As details can be found in that paper, only a brief account will be given here. The shaped-charge investigated in this work used a 62 mm diameter, 49° conical copper liner. Two flash X-ray radiographs of the broken jet were taken at 200 µs and 250 µs after the explosive was initiated. These radiographs provide the length *l*, the diameter *d*, the volume, the abscissa and the velocity of each fragment. Further analysis allows a kinematic description of the jet, including the evolution in time of its radius, even before breakup. It also provides the mean characteristics of the fragmentation process: velocity difference between fragments, final aspect ratio and breakup time versus fragment velocity. An average value of the aspect ratio $l/d \approx 4.25$ and a fragment – dependent breakup time in the range 110–170 µs are obtained. A plot of the reconstructed fragment velocity vs. cumulated fragments length is given in Fig. 5.

Rugosity measurements were carried out on recovered slugs stuck in the target. Only the rear part of the fragments, free of any contact with the target, was used. The rugosity was found to be rather homogeneous along the surface, and could be averaged to 14 µm. Scaled with respect to the estimated initial jet radius 2.5 mm, this leads to the order of 0.005 for the initial imperfection measure *a(0)*.

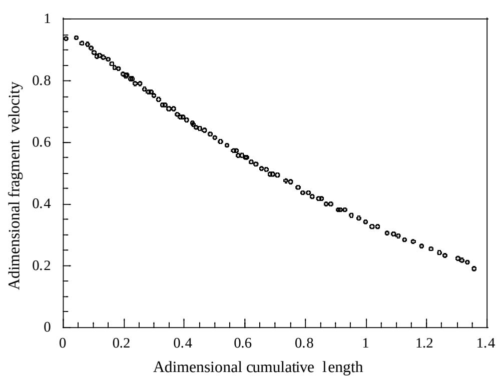

Figure 5: Fragment velocity vs. cumulated fragments length.

An initial strain rate of the order of $V/L \cong 10^4\ s^{-1}$ is used. The perturbation meeting the breakup criterion $a(t_b) = 1$ sooner than any other leads to the breakup time $t_b = 132$ µs. By the time the jet breaks up, the corresponding perturbation wavelength has evolved to the final aspect ratio 4.47. The calculated breakup time and final aspect ratio are therefore compatible with the experimental data: $t_b = 110$–170 µs and $l/d \cong 4.25$.

CONCLUDING REMARKS

This good agreement shows that the model has the ability to yield the right orders of magnitude for the main breakup characteristics, when a plausible set of material data and of initial / boundary conditions is used. Thus it seems to retain the essential features for a basic understanding of the phenomenon, i.e. radial inertia and a two-dimensional formulation of viscoplasticity (with a low strain rate sensitivity). However, the particulation process is clearly more complex, and a host of different factors should be taken into account for a more refined modelization. Among the latter are the non-uniformity of the initial configuration of the jet, the microstructure of the liner material, the thermal coupling and breakup mechanisms. The influence of the material microstructure can be investigated by using the model via the Hall-Petch law, as well as the initial jet non-uniformity. The assessment of the model predictions would then depend on more extensive material and experimental data.

REFERENCES

1. G. BIRKHOFF, D.P. MACDOUGALL, E.M. PUGH and G.I. TAYLOR, Explosives with lined cavities, *J. Appl. Phys.*, 19, 563–582, 1948.
2. R.J. EICHELBERGER and E.M. PUGH, Experimental verification of jet formation by charges with lined conical cavities, *J. Appl. Phys.*, 23, 537–542, 1952.
3. P.C. CHOU and J. CARLEONE, The stability of shaped-charge jets, *J. Appl. Phys.*, 48, 4187–4195, 1977.
4. E. HIRSCH, A formula for the shaped-charge jet breakup time, *Propellants and Explosives*, 4, 89–94, 1979.
5. J.P. CURTIS, Axisymmetric instability model for shaped charge jets, *J. Appl. Phys.*, 61, 4978–4985, 1987.
6. I. FRANKEL and D. WEIHS, Stability of a capillary jet with linearly increasing axial velocity (with application to shaped charges), *J. Fluid. Mech.*, 155, 289–307, 1985; Influence of viscosity on the capillary instability of a stretching jet, *J. Fluid. Mech.*, 185, 361–383, 1987.
7. L.A. ROMERO, The instability of rapidly stretching plastic jets, *J. Appl. Phys.*, 65, 3006–3016, 1989.
8. R.R. KARPP, L.M. HULL and M.L. PRICE, A technique for estimating the strength of materials in stretching shaped-charge jets, *Proc. of 15th International Symposium on Ballistics, Jerusalem*, 175–182, 1995.
9. V. JEANCLAUDE and C. FRESSENGEAS, Breakup of high speed metallic jets: the influence of nonlinear viscosity, *Proc. of Am. Soc. Mech. Eng. FEDSM00, Boston*, 11283, 2000.
10. P.S. FOLLANSBEE, G. REGAZZONI, U.F. KOCKS, Dislocation kinetics at high strain rates, *Acta Met.*, 35, 2865–2875, 1987.
11. C. FRESSENGEAS and A. MOLINARI, Inertia and thermal effects on the localization of plastic flow, *Acta. Met.*, 33, 387–396, 1985.
12. J.W. HUTCHINSON and K.W. NEALE, Sheet necking I, II, III *in Mechanics of sheet metal forming, Material Behavior and Deformation Analysis* (Ed. D.P. Koistinen, N.M. Wang), Plenum Press, New-York – London, 1978.
13. J.W. HUTCHINSON and H. OBRECHT, Tensile instabilities in strain-rate dependent materials, *Proc. of Fracture 1977, ICF4* (Ed. D.M.R. TAPLIN), 1, 101, Waterloo – Canada, 1977.
14. J. PETIT, Fragmented jet analysis and its use, *Proc. of 16th International Symposium on Ballistics, San Francisco*, 473–482, 1996.